UNCLASSIFIED

[redacted]

[redacted]

Technical Report No. 32-835

An Experimental Feasibility Study of Injectant Materials to Alleviate Mars Entry Communications Blackout

(Title Unclassified)

Arnold J. Kelly

D. R. Bartz, Manager
Propulsion Division

Copy No. 298

Classification Changed to
UNCLASSIFIED
Authority
E. O. 11652
Date 1/4/73
E. Talamantes

JET PROPULSION LABORATORY
CALIFORNIA INSTITUTE OF TECHNOLOGY
PASADENA, CALIFORNIA

November 15, 1965

UNCLASSIFIED

[redacted]

UNCLASSIFIED

UNCLASSIFIED

UNCLASSIFIED

Copyright © 1965
Jet Propulsion Laboratory
California Institute of Technology

Prepared Under Contract No. NAS 7-100
National Aeronautics & Space Administration

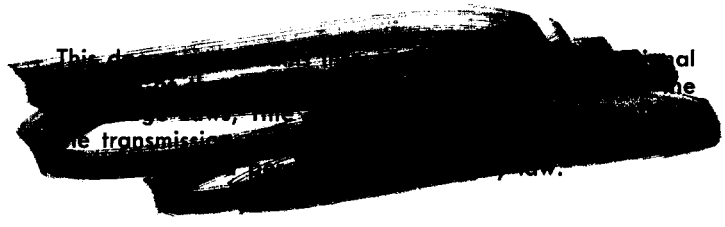

UNCLASSIFIED

CONTENTS

I. Introduction 1

II. Simulation of Martian Entry Conditions 2

III. Experimental Arrangement 3
A. Injectant Flow System 3
B. Microwave Swinging Probe 4

IV. Interpretation of Microwave Data 6
A. Microwave Idealized Theory 6
B. Microwave Circuitry Operation 6
C. Microwave Experimental Data 7
D. Corrections to the Microwave Theory 7

V. Selection of Quench Gases 9
A. Comparison Tests 9
B. Evaluation of Injectant Gases 10

VI. SF_6 Tests 11
A. Test Data: $\ell = 49.6$ cm 11
B. Test Data: $\ell = 99.4$ cm 11
C. Estimate of Electron Temperature 12
D. Electron Density vs Flow Rate 12
E. Efficiency of SF_6 as Electrophilic Material 12
F. Spacecraft Utilization Implications 13

VII. Summary and Conclusions 14

References 14

TABLES

1. Comparison of physical characteristics of MPD plume and capsule wake 2

2. Comparison of injectant gases 10

FIGURES

1. Schematic of experiment 4

2. MPD source in operation, SF_6 injected through plate 5

3. Theoretical plot of P_T vs n_e (for $m = 4.0$, $\omega = 2\pi \times 24$GHz, $\nu_c/\omega = 0.05$) 5

UNCLASSIFIED

FIGURES (Cont'd)

4. Microwave circuit diagram 7
5. Test record 8
6. Electron density profiles for various SF_6 flow rates, $\ell = 49.6$ cm 8
7. Electron density profiles, two test conditions, $\ell = 99.4$ cm 8
8. Electron density profiles for various SF_6 flow rates, $\ell = 99.4$ cm 9
9. Electron density vs SF_6 flow rate at two lateral positions, $\ell = 49.6$ cm 12
10. Electron density vs SF_6 flow rate at two lateral positions, $\ell = 99.4$ cm 12
11. Overall electron depletion rate vs SF_6 flow rate 13

ABSTRACT

A number of Mars-lander mission profiles currently under consideration involve atmospheric braking and, also, require that continuous communication be maintained with the spacecraft. For these missions to be successful, therefore, requires that some means be provided to reduce the debilitating effects of shock-produced ionization (expected to occur early in the entry maneuver) upon the fixed-frequency telemetry signal.

An experimental program has been initiated to establish the feasibility of using various appropriate materials, injected into the spacecraft wake, as a means of reducing the free-electron density level sufficiently to eliminate its interference with telemetry. It has been determined that the flow conditions (pressure, temperature, electron density) anticipated behind the bow shock of a blunt Martian entry body can be accurately simulated by the plume from an energetic magneto-plasmadynamic (MPD) arc source.

One such source, operating in a Laboratory vacuum facility, provides a large (~60-cm diam), steady, reproducible plume. Immersed in this plume, its upper surface parallel to, and some 6.35 cm below the centerline of the plume, is an aerodynamically clean flat plate, through which various electron-captive materials are injected normally into the stream. The electron density profile existing downstream of this plate, with and without the presence of injectants, is determined by the use of a swinging microwave diagnostic arm. This microwave system, operating at a frequency of 24 GHz, monitors electron densities in the range 0.2×10^{12} to 6×10^{12} cm^{-3} with a spatial resolution of ~5 cm.

Electron density profile data were obtained for various injectant materials. From these data, the most promising injectant material was selected and studied more extensively.

I. INTRODUCTION

It is currently envisioned that a capsule will be soft-landed on the surface of Mars sometime during the early 1970s. The use of aerodynamic braking as a means of eliminating a large portion of the ~7000 m/sec entry velocity is currently under active consideration. For this method of entry to be at all feasible, it is necessary that a number of system constraints be satisfied, not the least of which is continuous communications via direct link to

Earth (S-band, i.e., 2295 Mc) and/or an indirect link through the orbiting bus and thence to Earth (also, probably S-band). Consequently, it is necessary to consider the effects of shock-produced ionization on the characteristics of the wake and on the propagation of the telemetry signal as it traverses this wake.

Spencer (Ref. 1)—assuming an isothermal 180°K Martian atmosphere composed of 40% N_2, 30% CO_2, and 30% A, and exhibiting a surface pressure of 11 mb, a scale height of ~11 km and postulating a 3.3-m-diam entry capsule possessing a 0.2 slug/ft^2 ballistic coefficient—has shown that there would be between 5 and 10 sec of S-band communications blackout for vertical entry and between 10 and 29 sec blackout at an entry angle of 20 deg to the local horizon, for entry velocities between 6400 and 8100 m/sec. These computations were made employing the assumption of isentropic-frozen expansion of the gas from the stagnation region to the local ambient pressure existing in the wake. That is, the total electron population was assumed fixed. The electron density level in the stagnation region was calculated using an equilibrium thermo-chemistry and normal shock program developed previously at the Jet Propulsion Laboratory (JPL). Blackout was taken to occur whenever the electron density in the wake was equal to, or exceeded, the critical plasma frequency associated with the telemetry signal, viz., 10^{11} cm^{-3} for the S-band signal assumed in his study. Phase shifts of the signal caused by electron concentration below cut-off were not taken into account. Since it appears that these effects can have a detrimental influence on the ability of the Deep Space Network to track the capsule properly, the electron density at which plasma effects become of importance will be considerably lower than the critical density. This is reflected in terms of longer periods of blackout (partial or complete).

On the basis of *Mariner IV* data (Ref. 2), it now appears that the Martian atmosphere has a surface pressure of ~7 mb, a scale height of ~9 km, is predominantly composed of CO_2, and is isothermal at 180°K. While the low surface pressure poses some question as to the overall suitability of employing aerodynamic braking as a means of entry, these new data do not significantly alter the conclusion that S-band communications blackout will occur. The peak electron densities encountered entering the Martian atmosphere, as it is presently thought to exist, will now occur at ~35 km, rather than at the ~50 km, calculated on the basis of Spencer's work. However, the peak electron density in the wake (assuming frozen isentropic flow) will be in the same range calculated by Spencer, i.e., $10^{11} \rightarrow 10^{12}$ cm^{-3} for typical entry velocities (~7000 m/sec) and entry angles.

II. SIMULATION OF MARTIAN ENTRY CONDITIONS

Because the telemetry signal must traverse significant portions of the capsule's near wake, one would ideally want to duplicate the physical characteristics of this region as realistically as possible. Previous studies (Ref. 3) of the plume generated by a magneto-plasma-dynamic (MPD) source, operating on argon in the JPL plasma vacuum facility, indicated that the physical characteristics of the plume should provide a relatively accurate simulation of the conditions estimated to exist in the wake of a blunt Martian entry capsule. In Table 1, the pertinent physical characteristics of the plume of an MPD source, operated so as to most closely duplicate conditions to be experienced in the wake of a Martian entry capsule, are compared with the expected wake conditions. These wake conditions are those which, it is anticipated, would occur

Table 1. Comparison of physical characteristics of MPD plume and capsule wake

Parameter	MPD plume	Capsule wake
Velocity, (m/sec)	$400 \rightarrow 800$[a]	<3300
Mach number	$>\sim 1$	<5[b]
Electron density, cm^{-3}	$10^{11} \rightarrow 10^{12}$	$10^{10} \rightarrow 10^{12}$
Pressure, μ	$140 \rightarrow 160$	$6 \rightarrow 180$[c]
Electron temperature, °K	1000 ± 400	$800 \rightarrow 1300$
Atom temperature, °K	1000 ± 400	$800 \rightarrow 1300$
Composition	A	CO_2

[a] Computation is based on extrapolated magnetic velocity probe measurements.
[b] This is an upper limit, the average Mach number of the wake is probably closer to unity than to 5.
[c] Peak electron density is estimated to occur at an altitude at which the pressure is ~130μ.

during periods of maximum electron density and are, therefore, of greatest interest. These estimates were based on the latest *Mariner IV* data (Ref. 2) for the Martian atmosphere.

As is apparent from the Table, the simulation of Martian entry wake condition by the MPD plume is probably adequate, except for the matter of chemistry. Attempts to operate the MPD source on CO_2 were unsuccessful because of severe erosion problems. While it is anticipated that purely chemical processes would have little effect on the electron attachment process, since the state of the electron gas is the dominant factor, this particular facet of the entry problem was not simulated and should be investigated further.

III. EXPERIMENTAL ARRANGEMENT

Figure 1 is a schematic representation of the pertinent features of the experiment devised to evaluate various gaseous injectant materials. The experiment was conducted in the JPL Plasma Flow Research Laboratory. This facility consisted of a 2.1-m diam by 4.2-m vacuum tank, evacuated by a 140,000-l/min capacity pumping system. The tank pressure was a function of flow rate. At 0.30 g/sec argon flow through the source the background pressure (p_t) was $\simeq 160\mu$, at 0.1 g/sec, $p_t \simeq 85\mu$ and under no flow conditions $p_t \leqq 10\mu$.

The MPD source, using a 6.1-mm OD tungsten cathode and a 16-mm ID copper anode, operating at flow rates up to 0.30 g/sec and at a constant current level of 1600 amp, produced a plume having a detectable electron density concentration extending over radial distances in excess of 30 cm.

A. Injectant Flow System

Immediately downstream of the source at a distance selected so as to place it in a shock-free region[1] is an aerodynamically clean flat plate. This plate had a chord of 15 cm, was 61 cm in length, 2 cm at its thickest section, and was positioned so as to be 6.35 cm below the centerline of the plume. A single convergent nozzle (0.572-mm ID) centered on, and the exit port was coincident with, the upper surface of the plate that was used in all the experiments reported herein. The plate was originally designed so that an array of injection ports could be readily emplaced to enhance the distribution of the injectant. However, it was soon discovered that a single sonic injectant nozzle, injecting material normal to the plate and the stream velocity, was completely adequate for this purpose. This is consistent with the work of Spaid and Zukoski (Ref. 4) who have demonstrated that dispersal of gaseous injectant material from such an arrangement should be highly efficient in low Mach-number ($\sim$1) streams. All tests were restricted to gaseous materials to obviate the difficulties associated with either vaporizing and/or atomizing liquid injectants. In this context, it should be mentioned that the flow system associated with the injection nozzle was designed around the use of commercially available Fisher-Porter triflat flow meters. These flow meters were operated at a constant pressure of 760 torr and at approximately room temperature (22°C) in order to take advantage of the calibration data available for these devices. The injection nozzle pressure was in all instances less than the 760 torr, but higher than critical, i.e., the flow was always choked. The flow system (except the flow meters) was constructed of Inconel, so as to be compatible with a wide range of corrosive gases and was helium leak tested and shown to be leak free.

Two lines lead to the injection nozzle, one was used for the injectant flow and the other was connected to a pressure gauge, thus permitting the injectant pressure to be monitored. In each of these lines, a 3-way solenoid valve was connected to these lines where they emerged from the plate. In the unactivated position, these valves were open, i.e., the injectant and pressure lines had an unim-

[1]The injection hole in the plate was some 35.2 cm downstream of the exit plane of the MPD source.

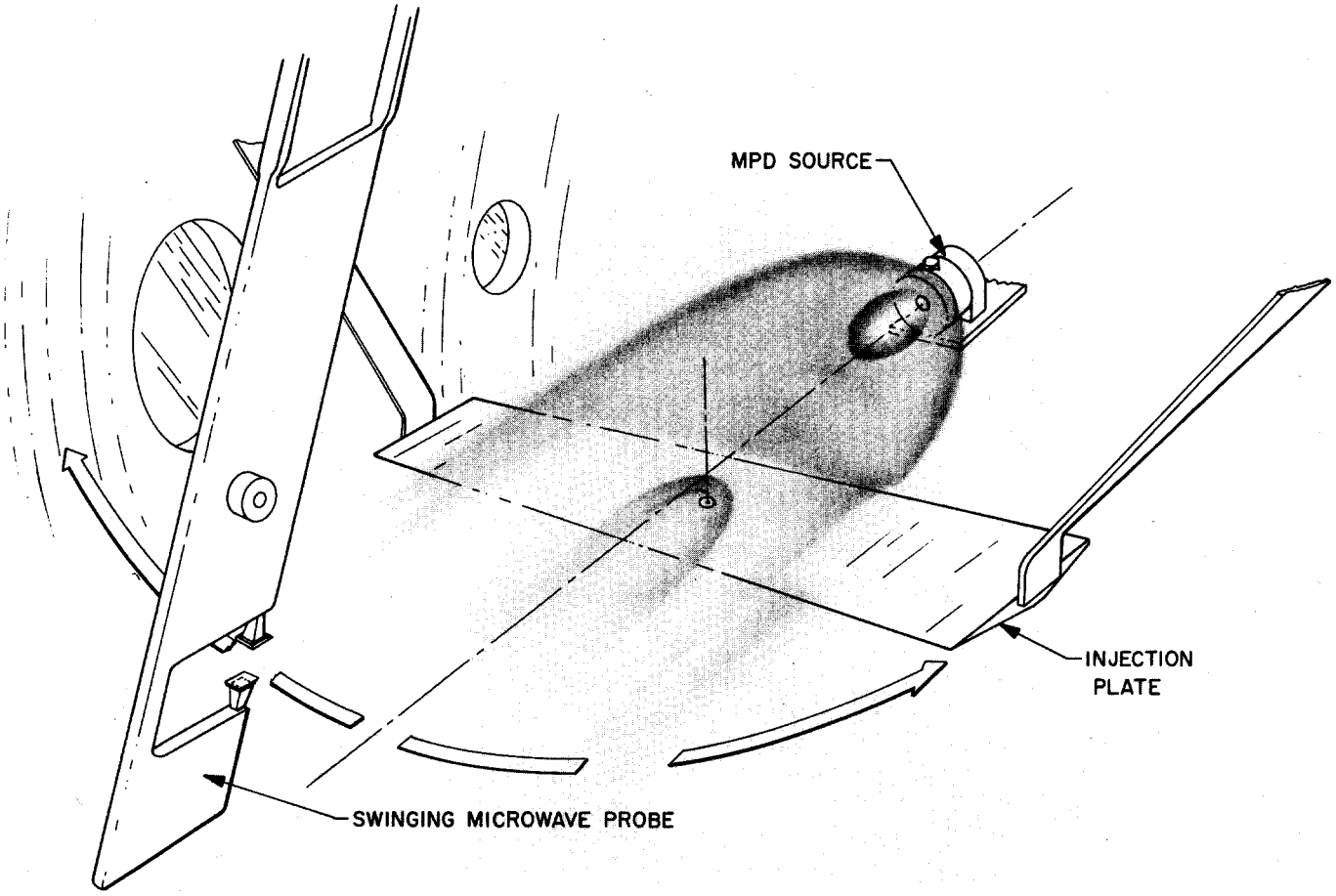

Fig. 1. Schematic of experiment

peded passage to the injection nozzle. When energized, the injectant feed line and the pressure sensing line were sealed off, while at the same time the ~30-cm portion of these lines between the valves and the injection nozzle were connected to a high vacuum pump that served to evacuate any material trapped in these lines which, otherwise, might dribble out of the nozzle and into the plume. In other words, the 3-way valves and the high-vacuum pump served to act as quick acting valves for the rapid termination of the injectant flow.

Figure 2, which is a photograph that was taken through one of the view parts of the vacuum facility, shows the plume from the MPD source as modified by the injection of SF_6.

B. Microwave Swinging Probe

Downstream of the injection plate, the swinging microwave probe (Ref. 5) describes a plane normal to the centerline of the plume. The longitudinal position of this plane with respect to the plate can be preadjusted as desired. The arm is normally latched to one side of the tank by means of a magnetic latching arrangement. Upon command, the arm is unlatched and swings so that the fixed gap formed by the microwave transmitting and receiving horns traverse an arc that passes through the centerline of the plume. Upon completion of the swing, the arm is automatically latched to the other side of the tank. The complete swing consumes approximately ½ sec. The microwave horns are covered with thin, quartz coverplates having sharp leading edges. While immersed in the plume, these coverplates delineate a shock-free slab of relatively homogeneous plasma. This permits an electron density profile to be obtained from the microwave data by application of the well documented theory (Ref. 6) of the interaction of a plane, plane-polarized electromagnetic wave with a homogeneous, isotropic slab of plasma, after suitable corrections have been applied.

The microwave circuitry used with this arm is shown in Fig. 3. Although capable of monitoring the measurable

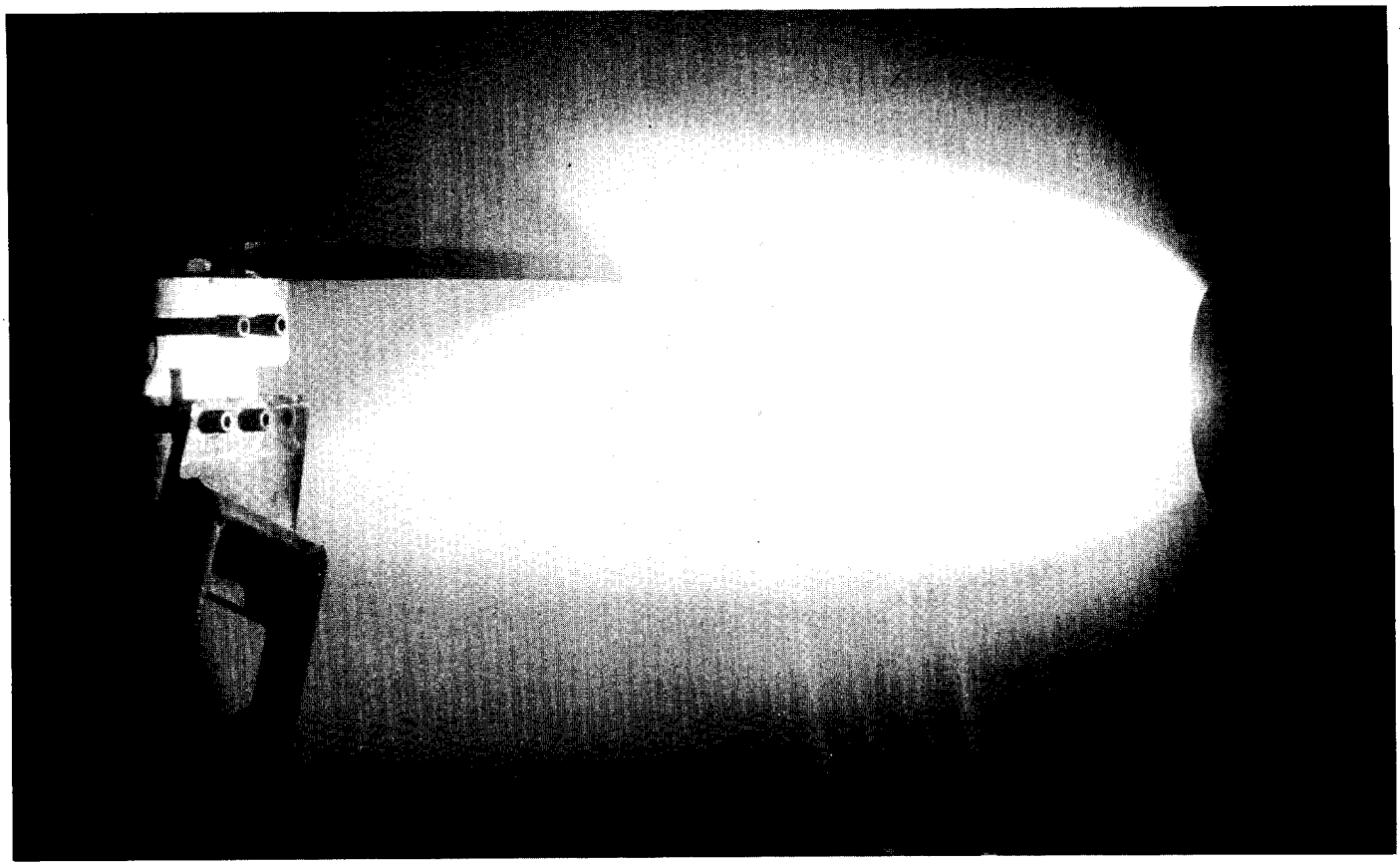

Fig. 2. MPD source in operation, SF_6 injected through plate

transmitted phase P_T, the measurable reflected phase P_R and the transmitted signal amplitude S_T, only the measurable transmitted phase P_T was utilized during these tests. Operating at 24 GHz, it was possible by use of the P_T signal, only, to detect electron densities in the range from 2×10^{11} to $\sim 6 \times 10^{12}$ cm^{-3}.

The angular position of the arm in the tank was sensed by a precision potentiometer, the output of which was used to control the horizontal deflection of an oscilloscope trace, the P_T signal being used to drive the beam vertically. In all cases the angular output from the potentiometer as recorded by the oscilloscope trace is related to the lateral position y of the center of the horn gap (i.e., the horizontal distance from the vertical plane encompassing the centerline of the plume). Because the arm swings in an arc 96.5 cm in radius, the change of elevation of the horn gap is small for lateral distances of interest (i.e., $y \leq 30$ cm). For $y = 30$ cm, the center of the horn gap is some 4.4 cm above the centerline.

In order to strike a reasonable balance between spatial resolution (where a narrow horn gap is desirable), and

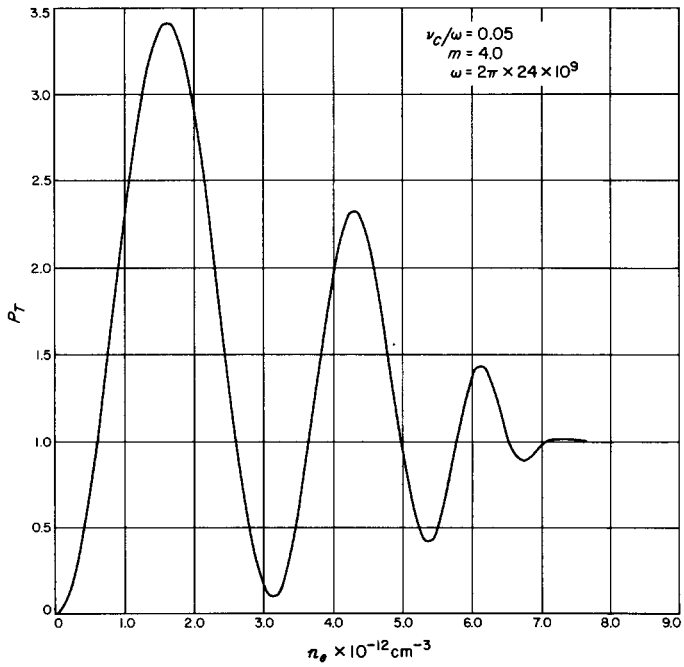

Fig. 3. Theoretical plot of P_T vs n_e (for $m = 4.0$, $\omega = 2\pi \times 24$GHz, $\nu_c/\omega = 0.05$)

sensitivity (where a wide horn gap is preferable) a gap width of $4\lambda_0$ (5 cm at 24 GHz) was chosen. Therefore, while the horn gap does sweep out an arc 96.5 cm in radius, for lateral distances of 30 cm or less, it is seen to travel what can be considered an approximate horizontal path.

Therefore, the two measurements of primary interest in this experiment were the injectant flow rates as determined by standard flow meters and the electron density profiles as measured by the swinging microwave probe.

IV. INTERPRETATION OF MICROWAVE DATA

A. Microwave Idealized Theory

As mentioned, while the microwave circuitry used with the arm (as depicted in Fig. 3) was fully capable of sensing the transmitted and reflected measurable phases (P_T and P_R) and the transmitted signal amplitude S_T, it was more convenient to use only one of the outputs, viz., the measurable transmitted phase P_T. The measurable transmitted phase is the output signal of an ideal square-law detector[2] in response to the vector sum of a suitably normalized reference wave and the wave that has traversed a region containing a plasma. By the vectorial summing of the E fields of the two waves and the suitable normalizing of the result, it is possible to write:

$$P_T = 1 + (S_T) - 2\sqrt{S_T}\cos\phi_T$$

where ϕ_T is the relative phase of the wave, which has traversed the plasma, with respect to the reference wave. The phase angle is normalized, such that for no plasma $\phi_T = 0$ and, since $S_T = 1$, then $P_T = 0$. If it is assumed that the plasma is a homogeneous, isotropic, plane slab of thickness $m\lambda_0$ (in our case, $m = 4$) characterized by the macroscopic parameters: electron density (n_e) and electron collision frequency (ν_c), and that the microwave signal can be represented as a plane, plane-polarized monochromatic wave, it is a straight-forward, albeit algebraically involved (Ref. 6), process to determine P_T as a function of n_e and ν_c/ω, where ω is the frequency of the microwave signal[3]. Figure 4 represents the results of such a computation for a plasma slab of thickness $4\lambda_0$ ($m = 4$), a value of ν_c/ω equal to 0.05, and a microwave frequency $\omega = 2\pi \times 24$ GHz.

B. Microwave Circuitry Operation

As in all measurements involving phase, it is necessary to maintain frequency to within narrow limits. In the experiments conducted using the measurable phase (P_T) circuitry of Fig. 3, it was possible by use of a standard klystron source (Raytheon 2K33) to maintain the frequency to within ± 3 MHz spread around the center frequency (24 GHz) for indefinite periods of time. A shift in frequency of ± 6 MHz was observed to produce measurable changes in signal level. All of the circuitry shown in the Figure was mounted inside of the vacuum facility and was arranged so as to allow the arm, and the circuit tied to it with rigid wave guide, to be moved easily in a longitudinal direction in the tank. This permitted a high degree of flexibility of operation insofar as microwave power, generated externally and fed into the tank via a bulkhead seal, could be readily transferred to the circuit through a length of flexible wave-guide.

Without the loop of wave guide shown in the reference leg of the circuit, which was used to compensate for the

[2]A square-law detector is a microwave detector whose electrical output is a linear function of the square of the E field of the incident microwave signal, in other words a linear output in response to the input microwave energy.

[3]It is to be emphasized that the microwaves respond to the free-electron concentration and only in a negligibly weak manner with the negative ions. In the formulation cited, the Longevin form for the electron equation of motion in response to the electromagnetic wave is employed.

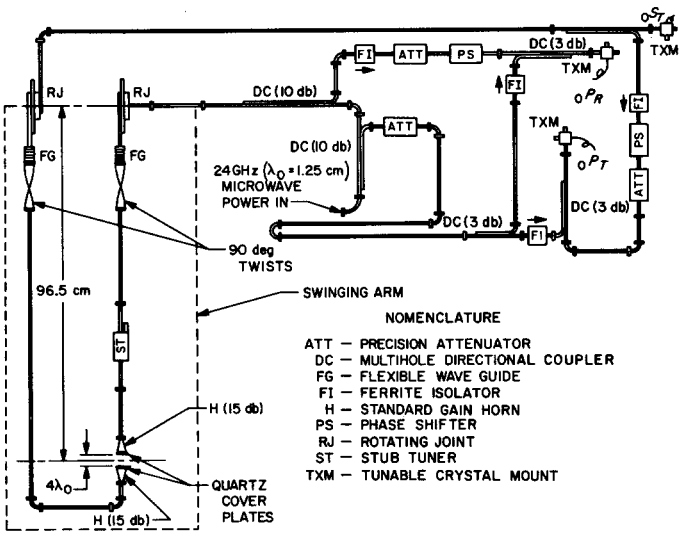

Fig. 4. Microwave circuit diagram

relatively long runs of wave guide necessary to duct the signal to and from the arm, it was found that if the circuit were balanced in air, it would be out of balance under vacuum conditions because of the difference in the dielectric constant of air and vacuum (~6 parts in 10,000). In fact, without the loop, the circuit acted as quite a respectable barometer. Once adjusted for a null in the P_T signal at zero n_e, the circuit proved to be remarkably unaffected by the vibration and shock produced when the arm latched and unlatched, and required no further adjustment. Because of heat soak in the tank from the operation of the MPD source, the reference loop and the wave guide on the arm (which was water-cooled) expanded at unequal rates. It was only possible to run the MPD source for periods of approximately one hour before a noticeable shift in the null of the P_T signal would become evident. This was a minor problem, since a considerable amount of data could be collected before the circuit heated to such a point as to necessitate shut down.

C. Microwave Experimental Data

Figure 4 shows the reproduction of a typical dual record taken with the swinging microwave arm, i.e., records of the P_T crystal detector output vs angular position of the arm. The narrow trace was recorded while SF_6 was being injected, and the broader trace was recorded after the injectant flow was cut off. The two traces were made on two consecutive swings of the arm. The displacement of the centers of the two traces was caused by backlash in the coupling between the arm and the potentiometer used to sense the arm's angular position. This served to displace the records, as seen, on two consecutive swings of the arm, so that in those cases where the profiles are quite similar (e.g., when relatively small amounts of injectant are used) the traces can be more easily interpreted.

D. Corrections to the Microwave Theory

Two corrections were applied to the microwave data: a correction for the crystal detector characteristics and a correction for the nonplanarity of the microwave beam between the horns. For all of the data collected during the course of the experiment, it was found that the indicated output of the 1N26 microwave crystal detectors, as recorded on the oscilloscope (denoted as $_0P_T$) could be related to the actual microwave energy (denoted as $_1P_T$) as determined by use of a precision calibrated attenuator (used to calibrate the crystal after each series of runs); by the empirical relation

$$\frac{{}_1P_T}{4} = \left(\frac{{}_0P_T}{4}\right)^{K_{P_T}}$$

For all of the calibrations, some 17 in number, K_{P_T} varied between 0.821 and 0.848, the average being 0.832. As the use of the mean K_{P_T} value to represent all the calibration data introduced, at most a 3% error, this was justified. For any one particular calibration, the individual calibration points were found to fall within 5% of the mean line for all values of $_0P_T$ recorded ($0.04 \leq {}_0P_T \leq 1.00$). The use of the crystal correction is essential for the proper interpretation of low $_0P_T$ data. Without such a correction, large (factors of 2 or more) errors in the electron density could be made.

The second correction that was applied to the idealized theory used to reduce the raw P_T data takes into account the fact that the transmitting and receiving horns are within each other's near-field pattern. That is, the transmitted wave is not ideally planar and, in spite of the fact that the quartz coverplates have been matched to the horns with a standing wave ratio of 1.05 or less, reflections in the horn-gap region still occur. The details of the field pattern correction are to be found in Ref. 7.

An IBM 7090 computer program was devised to make rapid calculations of electron density profiles from the data exemplified by the reproduced oscilloscope trace of Fig. 5. Both the crystal and field-pattern corrections were automatically applied in these computations. Because of the multivalued nature of P_T as a function of n_e (for a given ν_c/ω value), an additional criterion was involved

UNCLASSIFIED

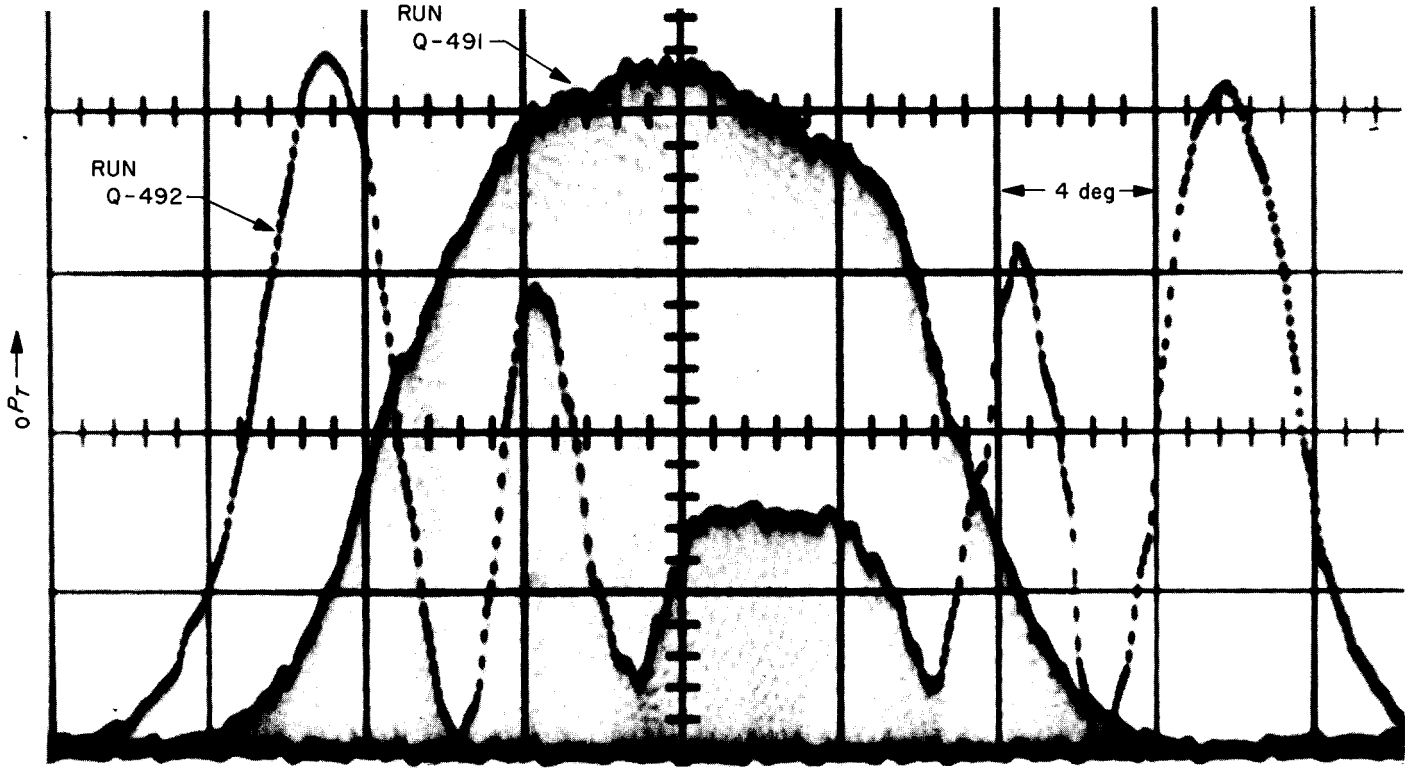

Fig. 5. Test record

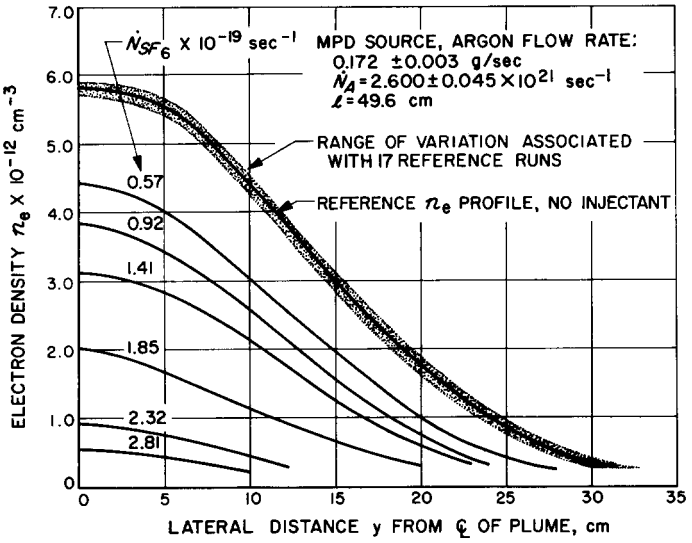

Fig. 6. Electron density profiles for various SF_6 flow rates, ℓ = 49.6 cm

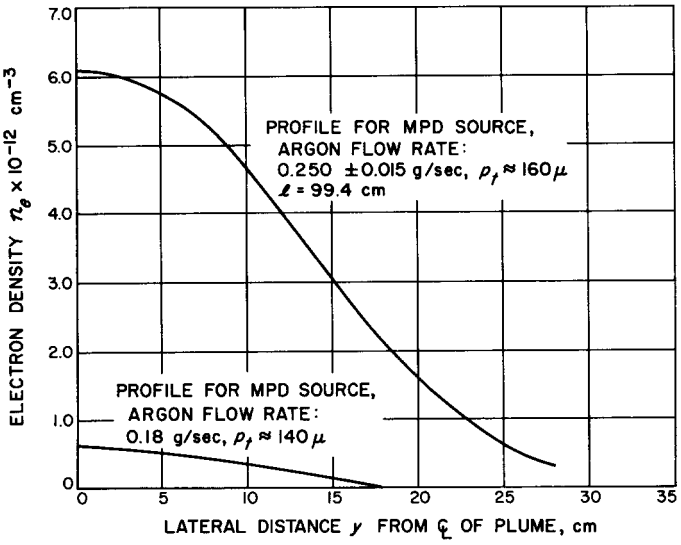
PROFILE FOR MPD SOURCE,
ARGON FLOW RATE:
0.250 ±0.015 g/sec, $p_f \approx 160\mu$
ℓ = 99.4 cm
PROFILE FOR MPD SOURCE,
ARGON FLOW RATE:
0.18 g/sec, $p_f \approx 140\mu$
ELECTRON DENSITY n_e x 10^{-12} cm^{-3}
LATERAL DISTANCE y FROM ℄ OF PLUME, cm

Fig. 7. Electron density profiles, two test conditions, ℓ = 99.4 cm

UNCLASSIFIED

in the step-by-step calculation of the electron density profile as a function of lateral position y, viz.,

$$\left(\frac{dn_e}{dy}\right)_{y=0} = 0$$

A corollary to this condition is that, in addition to n_e being a continuous function of y, the first derivative of n_e as a function of y also has to be continuous. This is reasonable when one considers the relatively high mobility of the electrons in the plasma, as well as the fact that the microwave probe provides a volumetric average of the electron concentration within a volume roughly $5 \times 5 \times 5$ cm.

No provision was made to account for the electron density gradient existing in the region of the horn gap. From previous work (Ref. 7), it is known that no significant influence concerning the interpretation of the microwave signal in terms of electron density should be anticipated for transverse gradients similar to those associated with the data of Figs. 6 through 8.

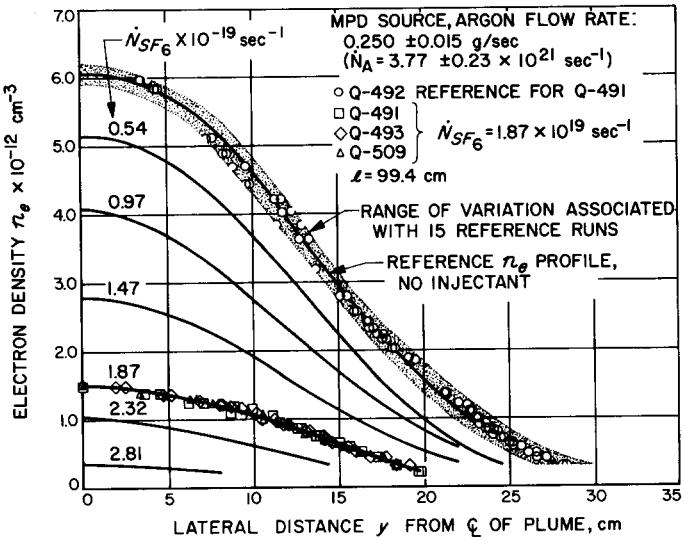

Fig. 8. Electron density profiles for various SF_6 flow rates $\ell = 99.4$ cm

V. SELECTION OF QUENCH GAS

A. Comparison Tests

The criterion used to select a candidate quench material was based on the relative flow rate necessary to cause a given reduction in electron density in comparison with a fixed standard (no-injectant) profile. This was easily accomplished by requiring that the standard electron density profiles, with and without injectant, have oscilloscope P_T vs angular position traces similar to those shown in Fig. 5. By making small corrections to the argon flow rate through the MPD source, it was possible to exercise precise control over the electron density profile; the higher the flow rate, the higher the peak electron density would be, with the source operated at a constant current level of 1600 amp. To gain some insight into the accuracy possible in reproducing a preferred electron density profile, reference should be made to Figs. 6 and 8. The shaded bands surrounding each of the reference profiles (no-injectant profiles) is the actual, observed variation for some 17 runs, in the case of Fig. 6, and 15 runs for Fig. 8. It should be mentioned that the MPD source proved to be quite stable in operation, only very small (<10%) variations in the flow rate being required over periods on the order of ½ hr to maintain the required profile. The electron density profile used as a standard for the case where quench gas was being injected corresponds to the curve labeled $N_{SF_6} = 1.85 \times 10^{19}$ sec^{-1} in Fig. 6.

All of the comparison runs were made at a position where the centerline of the microwave horns intersected the plume centerline at a distance $\ell = 49.6$ cm downstream of the injection nozzle. The test record shown in Fig. 5

was recorded when the arm was at a position $l = 99.4$ cm downstream of the injection nozzle. Although its appearance is virtually identical to those records used in the comparison tests, the particular data shown form part of the detailed evaluation of SF_6, which will be discussed subsequently. The record is one of three taken under identical injectant-flow conditions and is used, in addition to representing the standard comparison data, to demonstrate the reproducibility of electron density profiles when quench gases are being injected.[4]

The mode of operation was as follows. Once a preselected injectant flow rate was established, the arm was actuated and a profile was recorded. The solenoid values were then activated and the flow to the injection port was cut off. It was observed, particularly in the case of SF_6, that considerable luminosity would persist in the vicinity of the injection port. This luminosity, apparently due to injectant in the boundary layer of the plate, usually persisted with diminishing intensity for up to 20 sec. It was found that, if an electron density profile were to be recorded at times less than 30 sec after the actuation of the solenoid valves, the influence of the injectant could still be observed. Therefore, the reference profile (i.e., no-injectant) accompanying the injection run (both profiles were recorded on the same film) was made[5] 30 sec after the injection profile.

The operation of the MPD source was sufficiently stable, as discussed previously, to permit this mode of operation. Very little change could be discerned between succeeding reference runs, since noticeable changes took upward of ½ hr to become manifest. After the two (reference and injectant) profiles were recorded, the photograph of the oscilloscope traces was studied and the injectant and/or MPD source flow rate was adjusted to yield a record similar to that shown in Fig. 5.

To facilitate these comparison tests, a small amount of variation from the desired form of injection profile was deemed acceptable. In the desired injection profile the P_T signal trace is seen first to increase to the first peak of the P_T vs n_e characteristic (see Fig. 5, Run Q-491) and then to decrease symmetrically as the arm traverses the complete plume. This corresponds to an electron density profile having a peak[6] of $\sim 1.6 \times 10^{12}$ cm^{-3}. Records where the injection P_T trace exhibited a slight dip in the center (representative of, at most, a peak electron density[6] of 2.0×10^{12} cm^{-3}) were also used. This, of course, introduced some uncertainty into the evaluation procedure which, coupled with the slight variation of the reference profile, amounted to an estimated 30% overall uncertainty in the injectant flow rate used to characterize each of the gases tested.

[4]No multiple comparison run data are available at the 49.6-cm position for SF_6.

[5]For SF_6, a delay of 90 sec was found to be necessary.

[6]These maximum electron densities should be compared with the maximum of the reference profile which occurred at $\sim 6 \times 10^{12}$ cm^{-3}. Therefore, the comparison tests were run on the basis of at least a 3:1 reduction in peak electron density.

B. Evaluation of Injectant Gases

Table 2 represents the evaluation of the various gaseous injectant materials tested using the aforementioned procedure. As will be noted, these materials are listed in order of decreasing efficiency as determined by particle flow rate, $\dot{N}$. For comparison, the absolute mass flow rate ($\dot{m}_i$) and the ratio of injectant to MPD source argon flow rate ($\dot{m}_i/\dot{m}_A$) are also listed. For these tests the MPD source flow rate was in the range of 0.17 to 0.21 g/sec corresponding to tank pressures P_t of from ~ 140 to $\sim 150\mu$.

Argon was used as an injectant and was found to cause a diminution in the electron density profile that was consistent with a simple dilution of the plume gas. This result was substantiated by similar tests conducted with the microwave arm at a distance $l = 99.4$ cm from the injection port. To further verify this result, it was decided that another inert material would be injected. Dry nitrogen was selected for this test conducted at $l = 99.4$ cm. The surprising result that emerged from this very short series of tests was that nitrogen is apparently electronegative, even though N_2 has never been observed to form a negative ion (Ref. 8); the results indicate that possibly dissociation of the molecule occurs and that N^- is being formed.

Table 2. Comparison of injectant gases

Injectant	$\dot{N} \times 10^{-19}$ sec^{-1} [a]	$\dot{m}_i$ g/sec	$\dot{m}_i/\dot{m}_A$
SF_6	1.9	0.0045	0.026
Freon-12 (CCl_2F_2)	3.5	0.0070	0.038
Freon-13 ($CClF_3$)	4.0	0.0070	0.044
Freon-22 ($CHClF_2$)	5.2	0.0075	0.039
N_2O	5.6	0.0041	0.021
HCl	6.5	0.0039	0.019
HI	6.7	0.0142	0.083
HBr	7.1	0.0095	0.049
Cl_2	8.4	0.0099	0.050
NO	8.8	0.0044	0.021
O_2	13.3	0.0071	0.031

[a]The values of $\dot{N}$ should be considered as upper bounds, the lower bounds being an estimated 30% below the numbers listed.

These results, because they were obtained at a different station from that of the comparison tests, allow only a rough comparison to be made with the data of Table 2. For nitrogen, the same reduction in electron density as used in the comparison cases was obtained using $\dot{N} \simeq 8 \times 10^{19}$ sec^{-1}, $\dot{m}_i \simeq 0.004$ g/sec, $\dot{m}_i/\dot{m}_A \simeq 0.02$. This would indicate an electron quenching efficiency comparable to NO or Cl_2.

Using $\dot{N}$ as a basis of comparison, i.e., particle flow rate necessary to cause a fixed ($\sim$3:1) diminution in electron density, it is at once obvious, from Table 2, that SF_6 is a superior quench material. Because SF_6 is non-toxic, non-corrosive, and easy to handle, it would appear that it would be quite compatible with spacecraft usage. Therefore, a more elaborate series of tests were conducted, using SF_6 as an injectant.

VI. SF_6 TESTS

A. Test Data: $\ell = 49.6$ cm

The SF_6 injection tests were conducted basically in the same manner as the comparison tests, except that the SF_6 flow rate was varied over a sufficient range of values to cause almost complete elimination[7] of the electron density profile. Two series of tests were made, one with the microwave diagnostic probe at $\ell = 49.6$ cm, and the other with the arm at $\ell = 99.4$ cm. As in the comparison tests, once the SF_6 flow rate was established, the arm was actuated and the microwave profile recorded. The solenoid valves were then actuated and the injectant flow rate stopped. Ninety seconds later, the arm was again actuated to permit the reference (no-injectant) profile to be recorded. In Figs. 6 and 8, the shaded band around the reference profile represents the measured variation associated with some 17 tests, in the case of the 49.6-cm position (Fig. 6), and 15 tests, in the case of the 99.4-cm position (Fig. 8). These bands, it should be noted, include any random asymmetries present in the electron density profiles as the data for both sides are included in the half profile shown.

B. Test Data: $\ell = 99.4$ cm

The electron density profiles recorded at the 99.4-cm position were taken under slightly different circumstances from those recorded at 49.6 cm. In order to have approximately the same reference electron density profile at 99.4 cm as was observed at 49.6 cm, it was necessary to increase the argon flow rate through the MPD source from the $\sim$0.17 g/sec, used in tests at the 49.6-cm position, to $\sim$0.25 g/sec. In Fig. 7, reference (no-injectant) profiles recorded at the 99.4-cm position using two different MPD source flow tests are presented. The electron density profile recorded while the MPD source operated at roughly the flow rate employed in the tests conducted at 49.6 cm is seen to have a peak electron density that is approximately an order of magnitude lower than the reference profile associated with that flow rate at the 49.6-cm position. The increased MPD flow rate means that the electron density at the injection plate is necessarily higher for the 99.4-cm test series than it was for the 49.6-cm series in order to overcome the recombination and/or diffusion of free electrons out of the plume occurring in the interval between the two stations.

The raw data of Fig. 5 have been reduced[8] and are presented in Fig. 8, both halves of the profile being represented. Also included in this Figure are the reduced data from two other quench runs (Q-493 and Q-509) made at different times but at the same conditions as Run Q-491. The high degree of reproducibility of these data is evident. This justifies the lack of experimental data

[7]Because of the $\sim$30:1 electron density sensitivity range of the microwave probe, the minimum observable electron density profile had a peak electron density of $\sim$1/10 that of the reference (no-injectant) profile.

[8]The angular position (θ) of the arm recorded on the test record ($\theta = 4$ deg $\Rightarrow 1$ cm of the horizontal graticule) is related to the lateral position of the horn gap by the relation $y = 96.5 \sin \theta$ (cm).

points on Figs. 6, 7, and the remaining profiles of Fig. 8. In the majority of cases, there were two quench runs for each profile (i.e., two for each injectant flow rate), with the scatter of the data points falling within a band extending at most ±7% about the mean lines shown in these Figures.

C. Estimate of Electron Temperature

The profiles shown were reduced with an assumed ν_c/ω value of 0.05. This value of ν_c/ω provided the best fit to the data. The use of higher ($\nu_c/\omega \geqq 0.07$) or lower ($\nu_c/\omega \leqq 0.04$) values of ν_c/ω led to physically unrealistic discontinuities in the reduced electron density profile.[9] Previous work (Ref. 7) has indicated that the ν_c/ω data derived from the microwave probe can be accurately (±20%) related to Maxwell-averaged electron momentum-exchange cross sections. Because of the relatively low atom particle density and the relatively high ion density, the predominant electron momentum exchange collision would involve ions. From the measured electron density and collision frequency data using the coulombic cross section of Spitzer (Ref. 9) and the fact that the electron temperature is a weak function of radial position in the plume (Ref. 3), it was possible to infer that the electron temperature T_e was 1000°K ±400°K.

D. Electron Density vs Flow Rate

Cross plots of the profile data of Figs. 6 and 8 are displayed in Figs. 9 and 10, respectively, where the peak ($y = 0$) electron densities and the electron densities at $y = \pm 10$ cm for the 49.6-cm and 99.4-cm positions are shown. These graphs indicate an *approximately* linear decrease in electron density with increasing SF_6 flow rate. On the basis of the available data, a definitive statement as to the cause of the detailed behavior of these plots cannot be made. It is possible that the higher injectant flow rates have a tendency to disrupt the flow pattern sufficiently to cause a corresponding change in the electron density pattern or that equilibrium is being approached[10] leading to the tail-off in the curve.

E. Efficiency of SF_6 as Electrophilic Material

To determine the overall efficiency of SF_6 in regard to its ability to attach electrons, it is necessary to know both

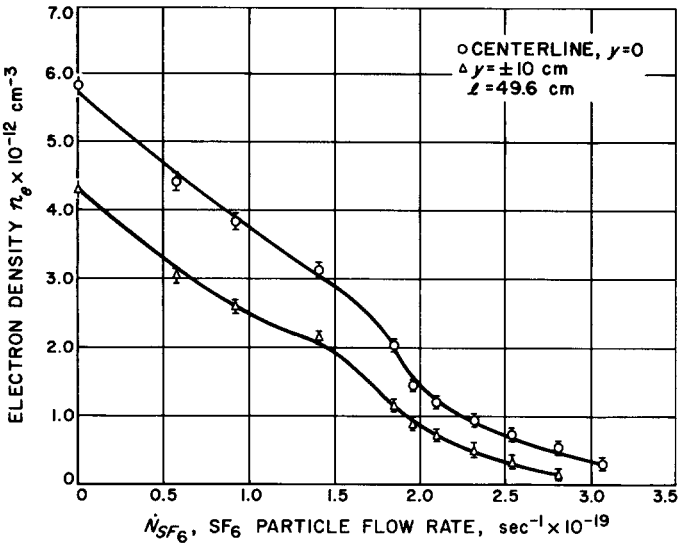

Fig. 9. Electron density vs SF_6 flow rate at two lateral positions, $\ell = 49.6$ cm

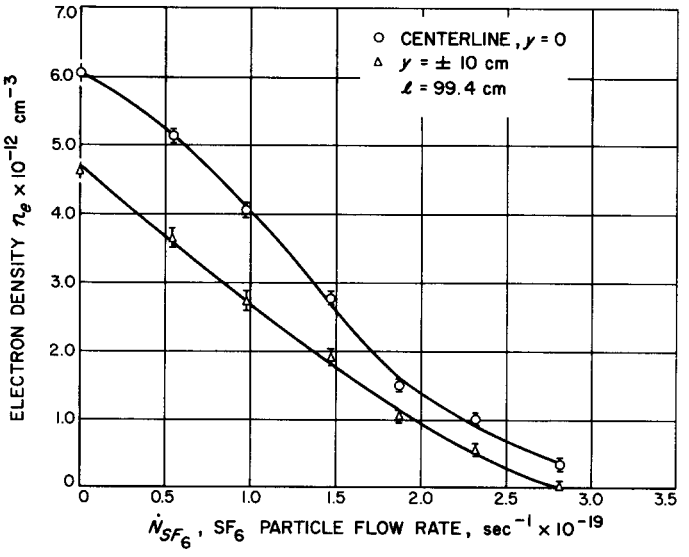

Fig. 10. Electron density vs SF_6 flow rate at two lateral positions, $\ell = 99.4$ cm

the velocity profile of the plume and the distribution of the SF_6 within the plume. In this preliminary study, no velocity profile measurements were made. However, from previous work (Ref. 3), it is reasonable to assume that the peak velocity of the plume was ~500 m/sec (this is consistent with a Mach 1 plume at ~1000°K), the profile[11] being gaussian with a half width of 11 cm. No species

[9]It should be noted that the accuracy of interpretation of the measurable phase data (when properly normalized) is relatively insensitive to the value of ν_c/ω that is assumed.

[10]That is, the rate of electron detachment from and ionization of the SF_6 is beginning to approach the rate of electron attachment.

[11]These data are consistent with magnetic velocity probe and impact probe measurements made of the plume without the injection plate in place.

UNCLASSIFIED [redacted]

distribution data were taken; therefore, no statement concerning the detailed distribution of the SF_6 can be made.

By integrating the product of the assumed velocity profile and the measured electron density profile over the area swept out by the microwave arm horn gap, it is then possible to determine the total number of electrons which have flowed in the period of 1 sec through the area swept out by the horn gap as it traversed the plume. By taking the difference between the number of electrons/sec that have flowed with no-injectant (reference profile) and the number that have flowed when SF_6 was injected, it is possible to arrive at the number of free electrons (per sec) which have been removed. This number (per sec) is denoted by $\Delta\dot{N}_e$. In Fig. 11, the results of this procedure as applied to the profiles of Figs. 6 and 8 are plotted. The results are remarkable, insofar as they show an approximately linear relation to exist between the number of

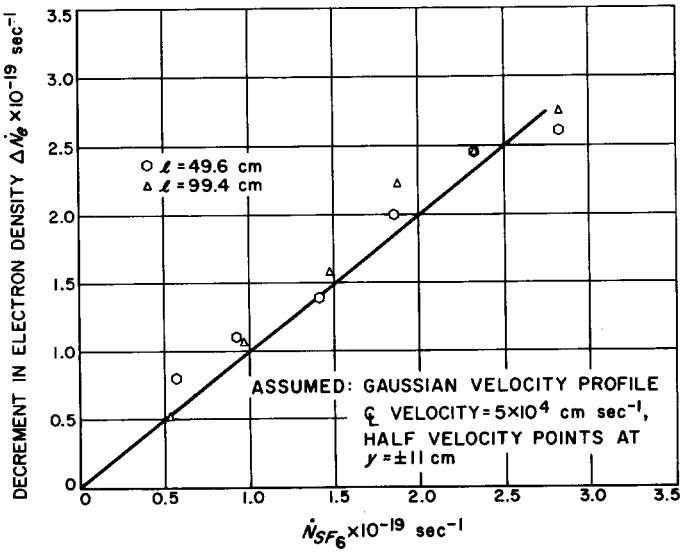

Fig. 11. Overall electron depletion rate vs SF_6 flow rate

depleted electrons and the number of SF_6 atoms used, the ratio being about 1:1. Note that without a mass spectroscopic survey, it is not possible to definitely determine where the SF_6 is dispersed. However, on the basis of these data, it is speculated that a substantial percentage of the injectant flow is, indeed, intercepted by the area delineated by the microwave horn gap. The velocity profile assumed was deemed to be reasonable on the basis of previous work. It is not likely that the peak plume velocity would be sufficiently lower than 500 m/sec or that the half velocity points would be narrower than ± 11 cm. Therefore, it is concluded that, to within an estimated error of $\pm 50\%$, each SF_6 molecule attaches one electron, and that the inverse processes are small by comparison.

F. Spacecraft Utilization Implications

Assuming that the SF_6 can be uniformly dispersed into the wake of the capsule and that the wake has a uniform electron density commensurate with frozen isentropic flow from the stagnation point, and further postulating that the volume of the wake (i.e., the region of high electron density) can be represented by the volume swept out by the capsule (the product of frontal area and capsule velocity), one can make some crude estimates of the total SF_6 required for complete elimination of free electrons from the wake. For a 4.2-m-diam capsule, using the electron density and velocity profiles calculated by Spencer (Ref. 1), (8110 m/sec entry velocity, entry angles between 20 and 90 deg to the local horizon, etc.), the total required SF_6 amounts to somewhat less than 600 g, the peak SF_6 flow rate amounting to less than 110 g/sec. This estimate was based on the observed electrophilic behavior of SF_6 (one SF_6 molecule required to attach one electron). Even if one were to apply a safety factor of 10 to compensate for uncertainties associated with the assumptions used, the total required weight of SF_6 is still a modest 6 kg.

VII. SUMMARY AND CONCLUSIONS

This experiment was designed specifically to provide base-line information concerning the feasibility of employing various gaseous injectant materials to alleviate the communications blackout problem anticipated during capsule entry into the Martian atmosphere. As such, it represents an engineering study, as opposed to a purely scientific endeavor, where the individual phenomena under investigation (e.g., the electron attachment process) are isolated and studied without the influence of other phenomena. In this study, the instrumentation was limited; therefore, it was not possible to isolate the individual processes at work, although it appears certain that electron attachment by SF_6 is the dominant mechanism for electron depletion. The results, represented by Figs. 6 and 8 through 11, include whatever vagaries of the injection system that might be present. Therefore, one can only state that, insofar as the elimination of Martian entry blackout is concerned, this experiment, a relatively complete simulation of the problem, has demonstrated that suitable materials are available to perform the necessary depletion of the electron density — at least for distances in the wake on the order of no less than a meter. It was also shown that SF_6 demonstrates high potential as a quenching material; approximately one SF_6 molecule is required to eliminate one free electron. The answers to the more complex questions concerning the detailed mechanisms of electron attachment and detachment and of particle dispersal will have to await the application of more elaborate instrumentation and an overall refinement of the experiment.

REFERENCES

1. Spencer, D. F., *An Evaluation of the Communications Blackout Problem For a Blunt Mars-Entry Capsule, and a Potential Method For The Elimination of Blackout,* Report No. 32-594, Jet Propulsion Laboratory, California Institute of Technology, April 15, 1964.

2. Kliore, A., Cain, D. L., Levy, G. S., Eshleman, V. R., Fjeldbo, G., Drake, F. D., "Occultation Experiment: Results of the First Direct Measurement of Mars Atmosphere and Ionosphere" (in "*Mariner IV* Measurements near Mars: Initial Results"), *Science,* Vol. 149, No. 3689, pp. 1243-1248, September 10, 1965.

3. Kelly, A. J., Nerheim, N. M., Gardner, J. A., "Electron Density and Temperature Measurements in the Exhaust of a MPD Source," Paper No. 65-298, presented at AIAA 2nd Annual Meeting and Technical Demonstration, San Francisco, July 26-29, 1965. (To be published in *AIAA Journal.*)

4. Zukoski, E. E. and Spaid, F. W., "Secondary Injection of Gases Into a Supersonic Flow," California Institute of Technology, Guggenheim Jet Propulsion Center, Pasadena, California (October 1963).

5. Kelly, A. J., "A Microwave Probe For Plasma Plumes," *AIAA Journal,* Vol. 3, p. 372, 1965.

REFERENCES (Cont'd)

6. Jahn, R. G., "Microwave Probing of Ionized-Gas Flows," *The Physics of Fluids,* Vol. 5, No. 6, p. 678, 1962.

7. Kelly, A. J., "Atom-Atom Ionization Mechanisms and Cross Sections in Noble Gases and Noble Gas Mixtures," PhD Thesis, California Institute of Technology, Pasadena, California, June 1965.

8. McDaniel, E. W., *Collision Phenomena in Ionized Gases,* John Wiley and Sons, Inc., New York, 1964.

9. Spitzer, L., Jr., "Physics of Fully Ionized Gases," *Interscience Tracts on Physics and Astronomy, No. 3,* Interscience Publishers, Inc., New York, 1956.